

Supporting Information

Synergistic polysulfide regulation and lithium deposition enabled by core-shell Ag/Ag₂S heterostructured fabric

Zicheng Wang^{‡,a}, Ao Jiang^{‡,a}, Xinman Chen^a, Chao Yu^b, Yuan Tian^{*,a}, Cheng Wang^{*,a}

a Institute for New Energy Materials and Low-Carbon Technologies, Tianjin Key Laboratory of Advanced Functional Porous Materials, School of Materials Science and Engineering, Tianjin University of Technology, Tianjin, 300384, P. R. China

b School of Materials Science and Engineering, Hebei University of Technology, Tianjin 300130, P. R. China

*Corresponding Author

tianyuan@email.tjut.edu.cn (Yuan Tian); cwang@tjut.edu.cn (Cheng Wang)

‡These authors contributed equally.

Number of Pages : 12

Experimental Section

Chemicals

All chemicals were employed as received, requiring no further purification, including Poly(vinyl alcohol) 1799 (PVA, 98-99%, Aladdin), Sodium chloride (NaCl, Ar, 99.5%, Aladdin), Thiourea ($\geq 99\%$, Aladdin), Silver nitrate (AgNO_3 , AR, Sinopharm), Polyacrylonitrile (PAN, Mw 150000, Picasso), N,N-dimethylformamide (DMF, AR, Kermel). Deionized water was used for all experiments.

Preparation of Ag/Ag₂S@NC, Ag@NC and NC

Firstly, 0.2 g NaCl and 1.3 g AgNO_3 was dissolved in 250 mL 0.75 wt% PVA aqueous solution under vigorous mechanical stirring for 1 h. Subsequently, the solution was poured into Teflon-lined stainless steel autoclave at 160 °C for 72 h. The resulting Ag@PVA was subjected to repeated washings with water and followed with vacuum freeze-drying. The product and thiourea were placed in the tube furnace under Ar atmosphere through partial sulfuration to obtain Ag/Ag₂S heterostructure nanofibers encased in carbon, while only annealing without thiourea was performed to obtain Ag metal nanofibers encased in carbon. Afterwards, Ag/Ag₂S@NC, Ag@NC and NC fabrics were synthesized by the electrospinning of PAN and heat treatment under Ar atmosphere. Here NC referred to nitrogen-doped carbon that carbonization of PAN.

Materials characterization

The X-ray diffraction (XRD) spectra were measured using a SmartLab 9 KW diffractometer. The scanning electron microscopy (SEM, Verios 460L) and high-resolution transmission electron microscopy (HRTEM, Talos F200 X) with elemental mapping were utilized to

investigate the morphological and structural characteristics. The elemental makeup and chemical valence of the samples were examined using X-ray photoelectron spectroscopy (XPS, ESCALAB250Xi).

Visualized LiPSs adsorption test

The blank electrolyte was composed of 1.0 M LiTFSI and 2 wt% LiNO₃ in a 1:1 (v/v) mixture of 1,3-dioxolane (DOL) and 1,2-dimethoxyethane (DME). The Li₂S₆ electrolyte was adopted in the visualized LiPSs adsorption test, that adding S and Li₂S (molar ratio 5:1) into blank electrolyte. The three pieces of circular discs (Ag/Ag₂S@NC, Ag@NC and NC) with 12 mm in diameter immersed separately in 10 mL Li₂S₆ electrolyte. After static adsorption, the supernatants were analyzed using an ultraviolet-visible (UV) spectrophotometer to evaluate the absorbability toward LiPSs.

Preparation of Li₂S₆ symmetric cells

The Li₂S₆ symmetric cell was assembled with the same electrodes (Ag/Ag₂S@NC, Ag@NC or NC circular disc for both the working and counter electrodes, and Li₂S₆ electrolyte. The cyclic voltammetry (CV) measurements from -1.5 V to 1.5 V were performed on a CHI-760E electrochemistry workstation, while electrochemical impedance spectroscopy (EIS) plots were tested for a frequency range of 0.1 Hz to 10⁵ Hz.

Linear sweep voltammetry (LSV) measurement

The LSV curves were carried out using a three-electrode system containing the working electrode (Ag/Ag₂S@NC, Ag@NC or NC circular disc), the counter electrode (platinum sheet) and the reference electrode (Ag/AgCl) with 0.1 M Li₂S/methanol solution.

Li₂S precipitation measurement

The Li_2S_8 electrolyte was synthesized by the addition of S and Li_2S (molar ratio 7:1) to the tetraglyme solvent. The coin cell was assembled with $\text{Ag}/\text{Ag}_2\text{S}@\text{NC}$, $\text{Ag}@\text{NC}$ or NC as the cathode, Celgard 2400 membrane and lithium foil as the anode. Notably, the Li_2S_8 electrolyte was applied to the cathode side, while the tetraglyme solution, devoid of Li_2S_8 was dropped on the anode side. The as-prepared batteries underwent galvanostatic discharging at a constant electric current of 0.112 mA to 2.06 V, followed by potentiostatic charging at 2.05 V to a current of below 10^{-5} A.

Assembly and measurements of the Li-S full batteries

The sulfur cathode was prepared by adding 40 μL 0.8 M Li_2S_6 electrolyte onto the $\text{Ag}/\text{Ag}_2\text{S}@\text{NC}$, $\text{Ag}@\text{NC}$ or NC circular disc, denoted as S- $\text{Ag}/\text{Ag}_2\text{S}@\text{NC}$, S- $\text{Ag}@\text{NC}$ or S-NC cathode. The sulfur loading was controlled to be approximately 5.4 mg cm^{-2} , while the corresponding electrolyte/sulfur (E/S) was around 6.5 $\mu\text{L mg}^{-1}$. For the lithium anode, the $\text{Ag}/\text{Ag}_2\text{S}@\text{NC}$, $\text{Ag}@\text{NC}$ or NC circular disc was separately electrochemically deposited 20 mAh cm^{-2} of Li to obtain Li- $\text{Ag}/\text{Ag}_2\text{S}@\text{NC}$, Li- $\text{Ag}@\text{NC}$ or Li-NC anode. All assembly procedures were performed in a strictly controlled argon glove box with an Ar and H_2O content of less than 0.1 ppm. The galvanostatic charge/discharge curves were conducted on the LAND CT3004A testing system. The CV curves were acquired using a CHI-760E electrochemical workstation at scan rates from 0.1 to 0.5 mV s^{-1} .

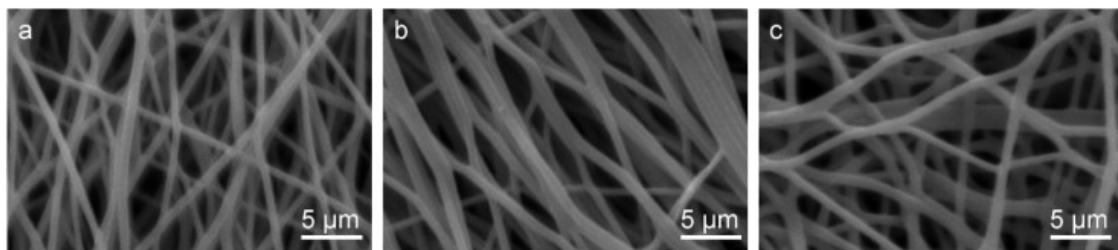


Figure S1. SEM images of (a) Ag/Ag₂S@NC, (b) Ag@NC and (c) NC.

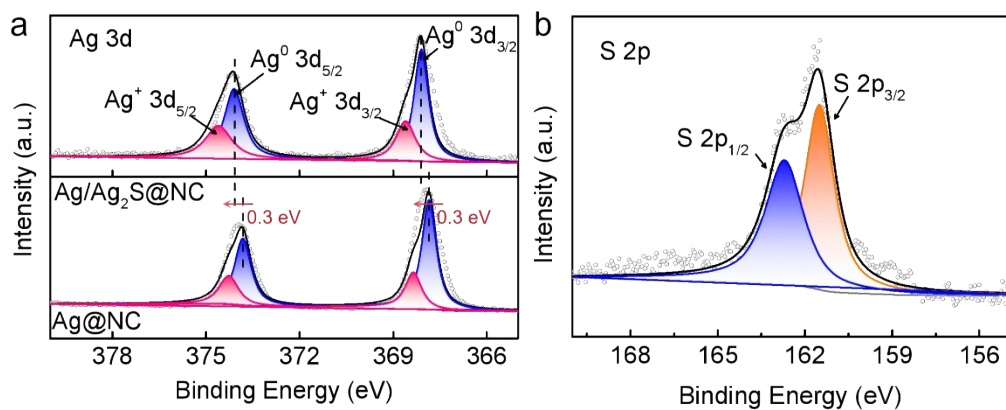


Figure S2. (a) Ag 3d and (b) S 2p high-resolution XPS spectra of Ag/Ag₂S@NC and Ag@NC.

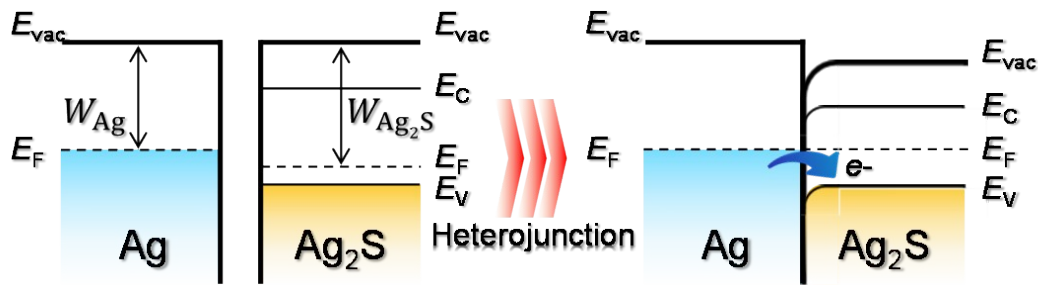


Figure S3. Simplified band structures in the Ag/Ag₂S system before and after contact.

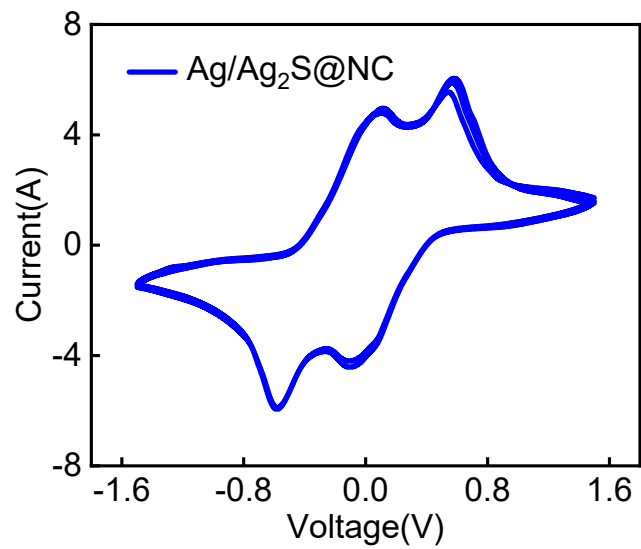


Figure S4. CV curves of Li_2S_6 symmetric cell with $\text{Ag}/\text{Ag}_2\text{S}@ \text{NC}$ electrode for several cycles.

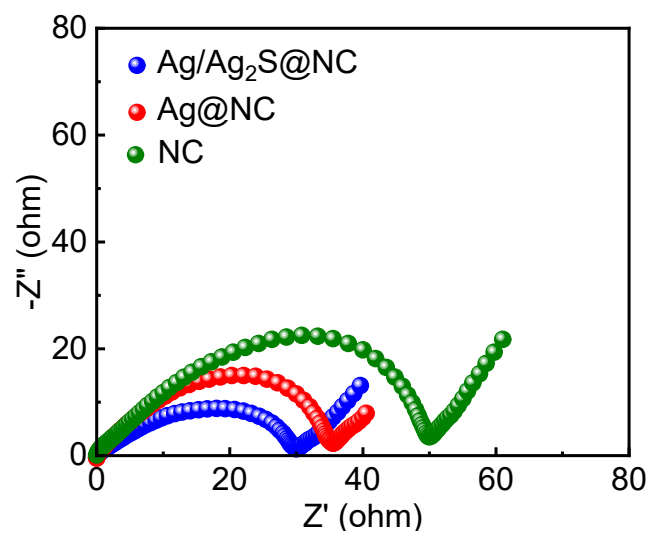


Figure S5. EIS plots of Li₂S₆ symmetric cells.

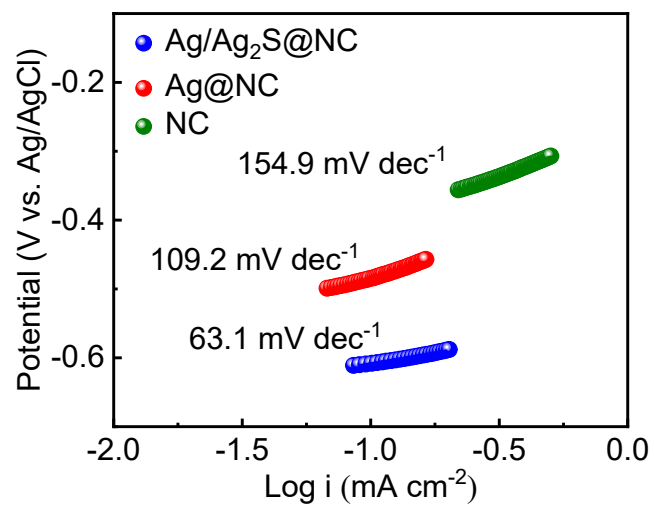


Figure S6. Tafel plots of the Ag/Ag₂S@NC, Ag@NC and NC electrodes.

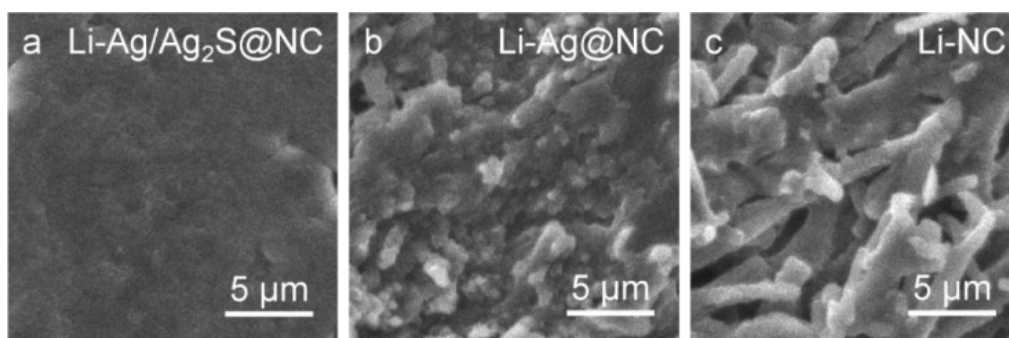


Figure S7. SEM images of (a) Li-Ag/Ag₂S@NC, (b) Li-Ag@NC and (c) Li-NC anodes upon 20 mAh cm⁻² of lithium deposition.

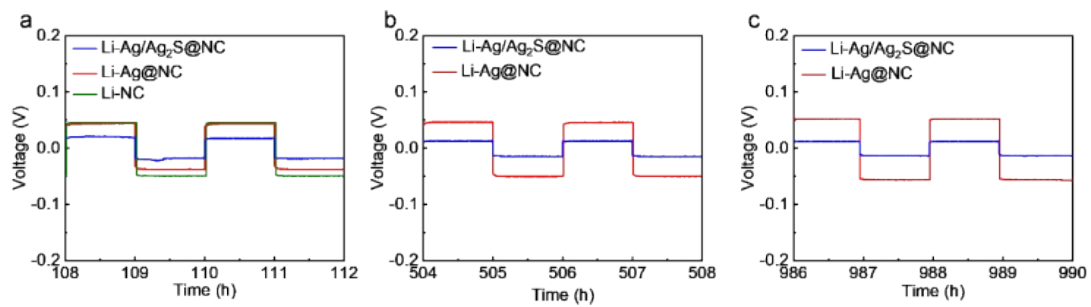


Figure S8. The voltage profiles of different Li||Li symmetric cells at 0.5 mA cm^{-2} for 0.5 mAh cm^{-2} .

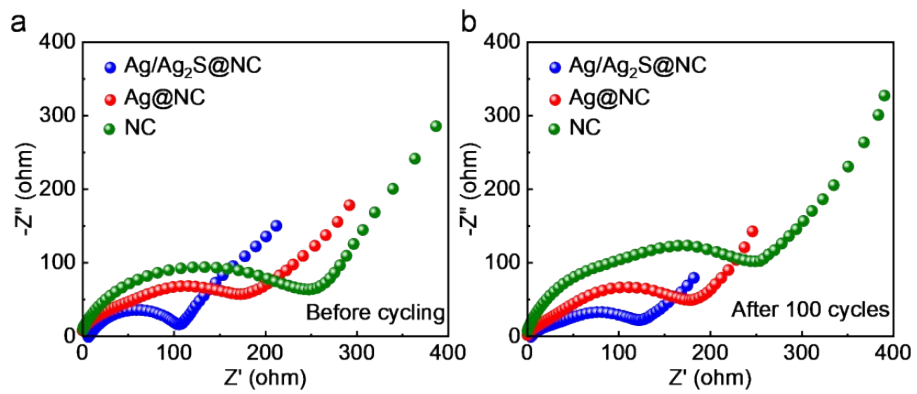


Figure S9. EIS plots (a) before cycling and (b) after 100 cycles at 0.5 mA cm^{-2} and 0.5 mA h cm^{-2} .

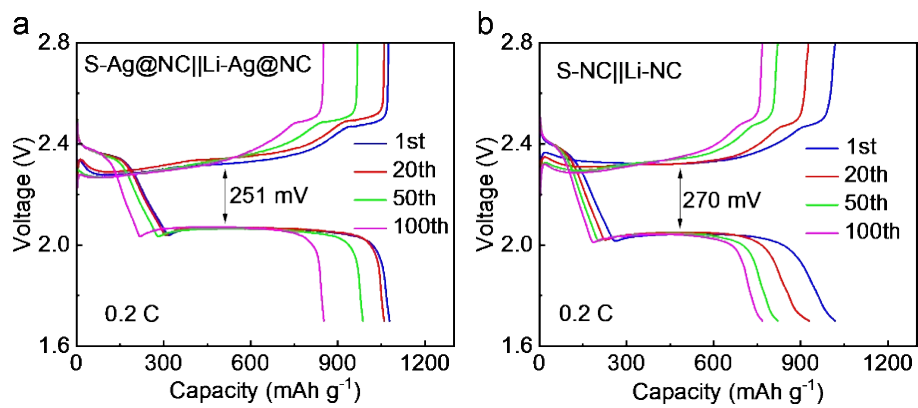


Figure S10. The charge-discharge curves at different cycles for (a) S-Ag@NC||Li-Ag@NC and (b) S-NC||Li-NC full batteries.

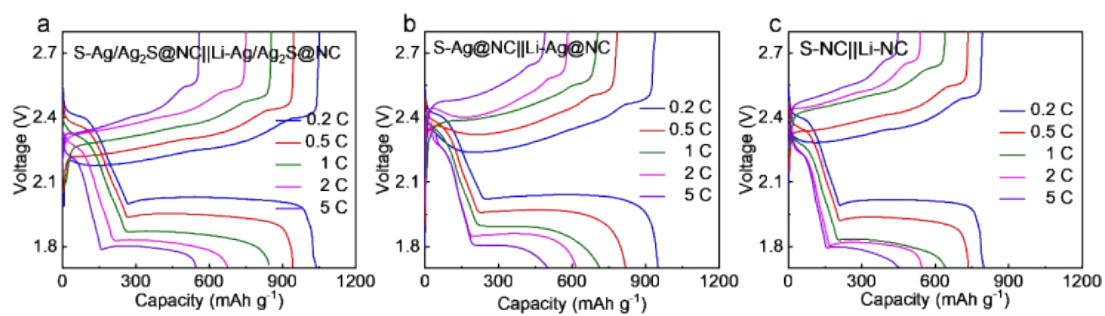


Figure S11. The charge-discharge curves at different rates of the (a) S-Ag/Ag₂S@NC||Li-Ag/Ag₂S@NC, (b) S-Ag@NC||Li-Ag@NC and (c) S-NC||Li-NC full batteries.

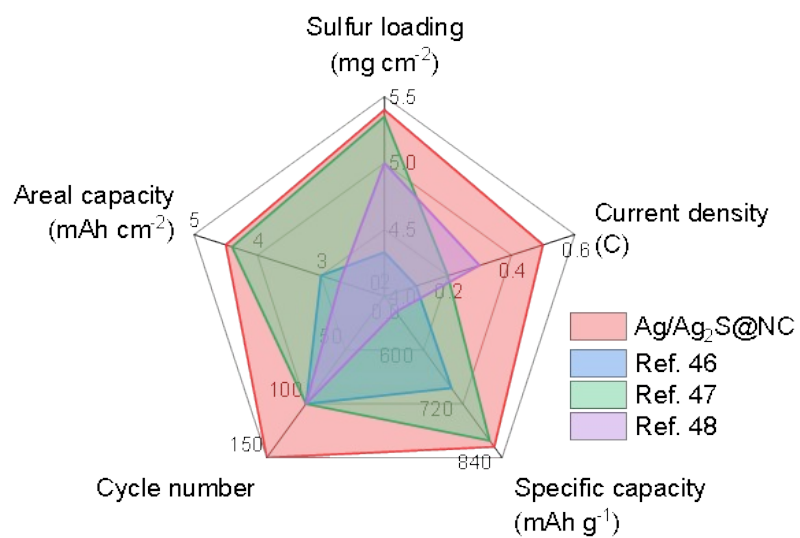


Figure S12. The radar chart of electrochemical performance for the Ag/Ag₂S@NC electrode with the other relevant materials.